ACS Photonics

Article

pubs.acs.org/journal/apchd5

Arbitrary Shape Designable Microscale Organic Light-Emitting Devices by Using Femtosecond Laser Reduced Graphene Oxide as a Patterned Electrode

Yan-Gang Bi,[†] Jing Feng,*[,†] Yun-Fei Li,[†] Yong-Lai Zhang,*[,†] Yu-Shan Liu,[†] Lu Chen,[†] Yue-Feng Liu,[†] Li Guo,[†] Shu Wei,[†] and Hong-Bo Sun[†,‡]

[†]State Key Laboratory on Integrated Optoelectronics, College of Electronic Science and Engineering, and [‡]College of Physics, Jilin University, 2699 Qianjin Street, Changchun 130012, China

ABSTRACT: Arbitrarily shape customized microscale organic light-emitting devices (micro-OLEDs) have been fabricated by using reduced graphene oxide (RGO) film as a patterned electrode. A femtosecond (Fs) laser was employed to fabricate the RGO electrode by direct reduction and patterning of the GO films according to preprogrammed patterns. The patterned RGO exhibits good conductivity for electrode applications in OLEDs. Various complex patterned micro-OLEDs were successfully created through this simple Fs laser fabrication process, which exhibit well-defined sizes, shapes, and edges and uniform electroluminescence characteristics. The arbitrarily shape customized micro-OLEDs open the door for new applications in microdisplays and three-dimensional or flexible displays.

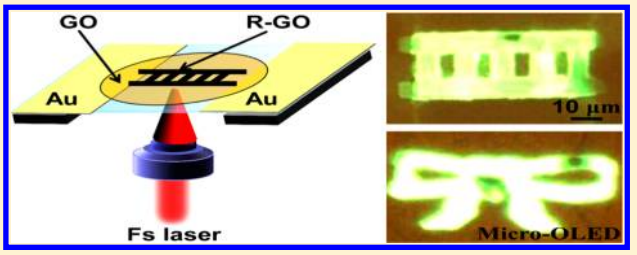

KEYWORDS: *reduced graphene oxide, microscale organic light-emitting device, patterned electrode, femtosecond laser direct writing, arbitrarily customized pattern*

Microscale organic light-emitting devices (micro-OLEDs) with fine designed patterns are required for the application of microdisplays or high-resolution diode matrices that will be used in three-dimensional (3D) and flexible displays.[1−3] The introduction of a microscale pattern onto the electrodes of the OLEDs is crucial in the development of the micro-OLEDs. The shadow mask method and various lithography-based technologies, such as the wet or dry etching process, can be used to pattern mirco- or nanoscale electrodes; however, they are up against the limitations of low resolution, high cost, or damage of the organic materials owing to the presence of oxygen or solvents.[3−7] Moreover, it is difficult to realize arbitrary shape in the microscale for most of the electrode materials, such as indium tin oxide (ITO) and metallic films, by using lithography-based technologies.[8−12] So far, a suitable fabrication technique for fabrication of the arbitrarily patterned micro-OLEDs with high resolution is still a challenge, which is an obstacle for the applications of micro-OLEDs.

Graphene, which features high electrical conductivity, high flexibility, good mechanical and thermal stability, and high optical transparency, has emerged as a new-generation electrode material, especially for organic electronic devices.[13−17] Graphene-based electrodes obtained from solution-processed reduced graphene oxide (RGO) have been applied in organic electronic devices, such as OLEDs, photovoltaics, photodetectors, and field-effect transistors.[18−23] Electrodes prepared from RGO require chemical or thermal treatment of GO to partially remove the oxygen-containing groups and to restore its electrical properties. Recently, femtosecond laser direct writing (FsLDW)-induced reduction of the GO has been reported, and the RGO can be synchronously patterned through the mask-free Fs laser nanowriting pathway.[15,24] FsLDW has been adapted as a nanoenabler due to its 3D processing capability, arbitrary designability, and reasonably high spatial resolution.[25−27] These features make it possible to pattern the GO films according to preprogrammed patterns. More importantly, its compatibility with the device fabrication process indicates a potential universality of this technique in fabricating micro-OLEDs. In this work, we have demonstrated that the direct reduction and patterning of RGO via FsLDW provides a simple and reliable technical route for the realization of micro-OLEDs with arbitrary shape customization. The micro-OLEDs employed FsLDW-induced RGO with a micro-pattern as the anode of the devices. The patterned micro-OLEDs with ladder and bowknot shapes were successfully created, which exhibit well-defined sizes, shapes, and edges and uniform electroluminescence (EL) characteristics.

RESULTS AND DISCUSSION

Figure 1a shows the preparative procedures of FsLDW-induced RGO as a patterned electrode of OLEDs. The GO was produced via a modified Hummers method from natural graphite and spin-coated on precleaned glass substrates. The Fs laser directly wrote on the GO film according to preprogrammed patterns, and then the reduced and patterned GO film

Received: April 4, 2014
Published: August 4, 2014

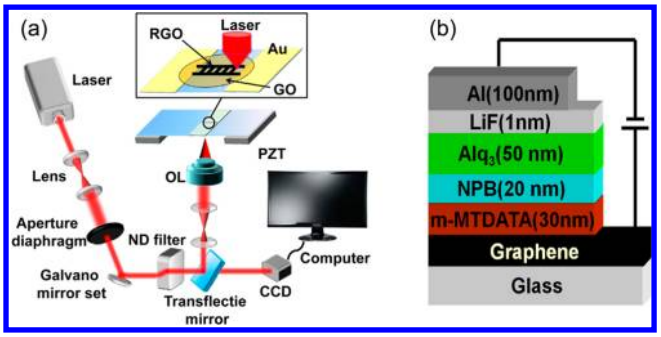

Figure 1. Illustration of the preparative procedure of FsLDW reducing and patterning the GO films (a) and schematic structure of an OLED based on FsLDW-induced RGO as a patterned electrode (b).

formed on the substrates as described in the Materials and Methods section and was used as the anode of the OLEDs.[15,24] Later, the micro-OLEDs based on the patterned and reduced GO anodes were fabricated with the structure RGO/m-MTDATA (30 nm)/NPB (20 nm)/Alq_3 (50 nm)/LiF (1 nm)/Al (100 nm) as shown in Figure 1b.

The surface morphology of the pristine GO and RGO was investigated by atomic force microscopy (AFM) (Figure 2).

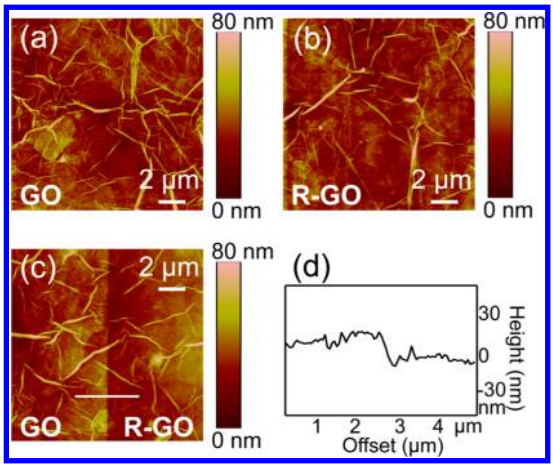

Figure 2. (a–c) AFM images of pristine GO and FsLDW-induced RGO and the height profile of the GO and FsLDW-induced RGO film along the white line (d).

The AFM image of GO films (Figure 2a) clearly shows GO sheets and some quasi-one-dimensional creases. The quasi-one-dimensional creases with a length scale of 0.1–1 μm and a height of 1–10 nm were formed by the overlap of GO sheets where some of the GO edges were scrolled or folded during film fabrication.[28,29] After reduction and patterning of the GO by the Fs laser, the root-mean-square (rms) roughness of the RGO film (Figure 2b) is decreased from 9.14 nm to 7.19 nm compared with that of a pristine GO film, which is significant for its application as an electrode in electronic or optoelectronic devices. The surface smoothness is proportional to the contact area between the electrode and the functional layers in the devices, and the smooth surface is beneficial to the electric charge injection. The thickness of the GO film decreases from 87 nm to 72 nm after FsLDW reduction, as shown in Figure 3. The RGO film with sunken surfaces could be clearly identified from the AFM images (Figure 2c). The sunken depth is about 15 nm, as can be seen in Figure 2d. The sinking of the RGO film should result from the mass loss of the GO films and as a

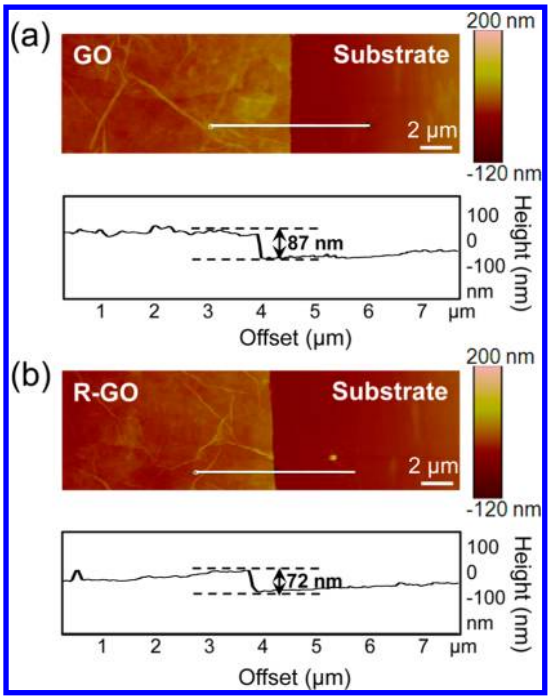

Figure 3. (a) AFM images of the edge of GO films and the height profile along the white line. (b) AFM images of the edge of FsLDW-reduced GO films and the height profile along the white line.

result of the rearrangement of atoms when the Fs laser beam enters and interacts with the GO film from the substrate side.[30] The nature of the mass loss is photochemical reduction, which has been discussed in detail in the literature.[15,31]

The reduction of the GO film by the FsLDW process can be determined by X-ray photoelectron spectroscopy (XPS). XPS results indicate that both pristine GO and laser-reduced RGO have signals of carbon and oxygen (Figure 4a). An initial XPS survey scan of GO reveals that the asymmetric C 1s peak can be fitted with three different peaks assigned to C–C (non-oxygenated ring carbon), C–O (hydroxyl and epoxy carbon), and C=O (carbonyl), respectively (Figure 4b).[24,32,33] The reduction degree of the GO is indexed by the atomic ratio of oxygen and carbon (O/C) obtained from taking the ratio of the C 1s peak areas in the XPS spectra. The O/C ratio of the pristine GO is 0.41, showing a high percentage of oxygen functionalities. After the FsLDW reduction, despite the fact that C–O and C=O bonds are also present in Figure 4c, the O/C ratio of the RGO deceases to 0.20, indicating the partial removal of oxygen. The electronic excitation effect and electron–hole recombination-induced thermal effect can decipher the mechanism of the oxygen removal in the laser reduction process. In the first several picoseconds of Fs laser reduction, the electronic excitation effect is significant. The excitation of electrons from bonding states to antibonding states under the laser effect could significantly weaken C–O electronic bonding near the top of the valence band and therefore lead to immediate oxygen removal. Later, a sufficient electron–hole recombination-induced thermal effect is dominant in the Fs laser reduction process on GO.[24]

To evaluate the conduction characteristics of the FsLDW-induced RGO film, resistivity and mobility of the RGO have been measured. The resistivity is 9.19×10^{-4} Ωm obtained by fabricating RGO microbelts between two electrodes. Bottom-gated field-effect transistors (FETs) with the RGO as a channel

dx.doi.org/10.1021/ph500106f | ACS Photonics 2014, 1, 690–695

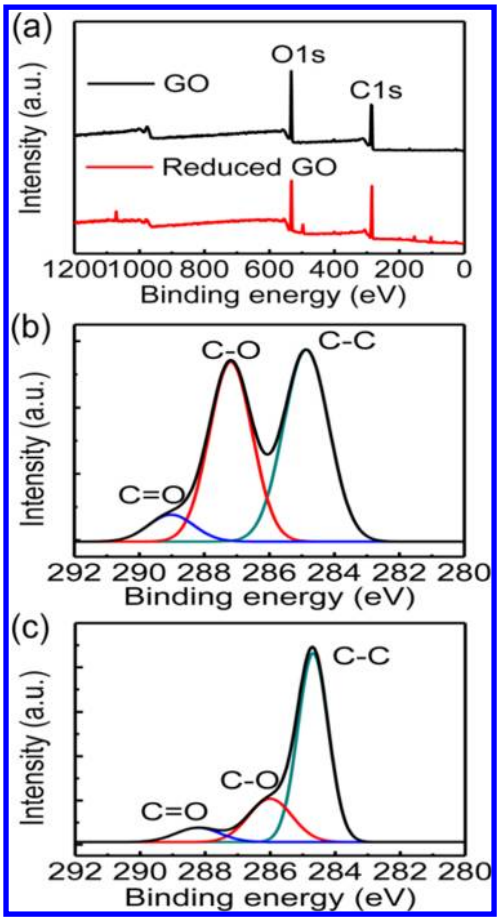

Figure 4. (a) Survey X-ray photoelectron spectra of pristine GO films and FsLDW-reduced GO films. C 1s XPS spectra of pristine GO films (b) and FsLDW-reduced GO films (c).

were fabricated to determine the mobility, as shown in Figure 5a–c. The FET was constructed with ITO as the gate and PMMA as the gate dielectric layer. GO film was spin-coated onto the PMMA layer, and a belt with a size of 35 × 75 μm^2 was reduced to RGO by the FsLDW as the channel between the source and drain Au electrodes. An RGO channel with the desired size and shape could be created freely and easily between two precoated electrodes by using the FsLDW technique. The GO film can be reduced to extend to the area under the Au electrodes since the FsLDW is processed from the bottom side of the FETs, so that a good ohmic contact between the source/drain electrodes and the RGO channel is expected. The output characteristics of the FETs with pristine GO and RGO as channels are compared and shown in Figure 5d and e. The pristine GO FET shows no gate effect (Figure 5d) due to its wide band gap and the high hole-injection barrier between the Au electrodes and the GO. The very small S/D current indicates that the carrier concentration is very low, and GO is insulating to some extent. Therefore, the influence of the pristine GO region in the RGO FETs is not taken into consideration on the grounds that it could be considered as part of the substrate due to its insulation property. Figure 5e shows representative output characteristics of the RGO FETs under different gate voltages in the range −80 to 80 V. The hole mobility of the bottom-gated RGO FET is estimated to be 0.36 $cm^2\ V^{-1}\ s^{-1}$ by the following equation:[20,24]

$$\mu = \frac{\Delta I_{ds}}{\Delta V_g}\frac{L}{WC_{ox}V_{ds}} \quad (1)$$

where $C_{ox} = \varepsilon_0\varepsilon_{PMMA}/t_{ox}$ is capacitance per unit area of the gate insulator; ε_0 is vacuum permittivity (8.85×10^{-12} F/m); ε_{PMMA} is the relative dielectric constant of PMMA (3.0); t_{ox} is the thickness of PMMA (200 nm); L and W are channel length (75 μm) and width (35 μm), respectively.

The fabricated micro-OLEDs with a green emission based on FsLDW-reduced and patterned GO electrodes are imaged using an optical microscope, and photographs of the operating devices under different driving voltages are shown in Figure 6. Ladder-shaped RGO was fabricated and used as the transparent anode of the micro-OLEDs. The micro-OLEDs show well-defined shapes and high resolution (Figure 6a). Light emission

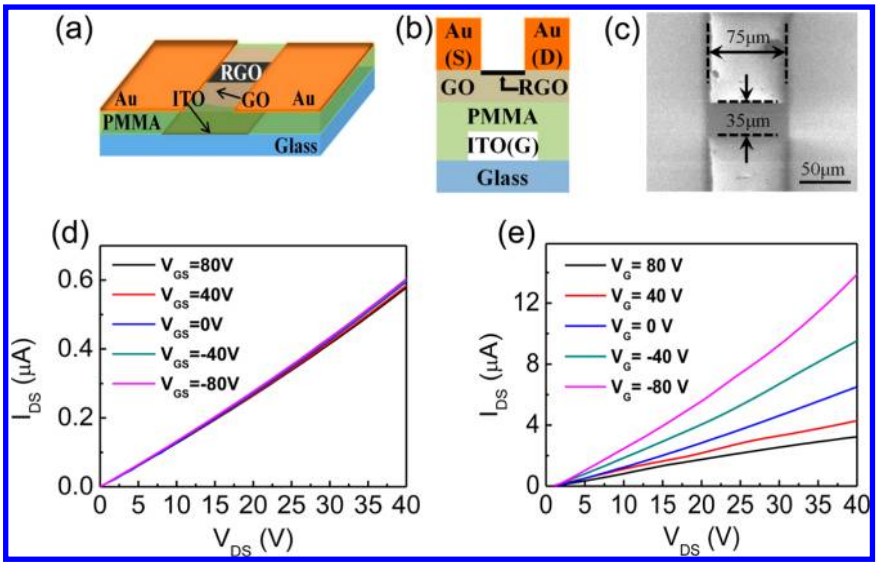

Figure 5. (a) Scheme of the bottom-gate RGO FET. (b) Cross-section schematic diagram of the FET. (c) SEM image of the FsLDW-reduced and patterned GO microbelt between source and drain electrodes as a channel. Output characteristics of FETs with GO (e) and FsLDW-reduced GO (f) as channels, respectively. The gate voltage is in the range −80 to 80 V.

dx.doi.org/10.1021/ph500106f | ACS Photonics 2014, 1, 690–695

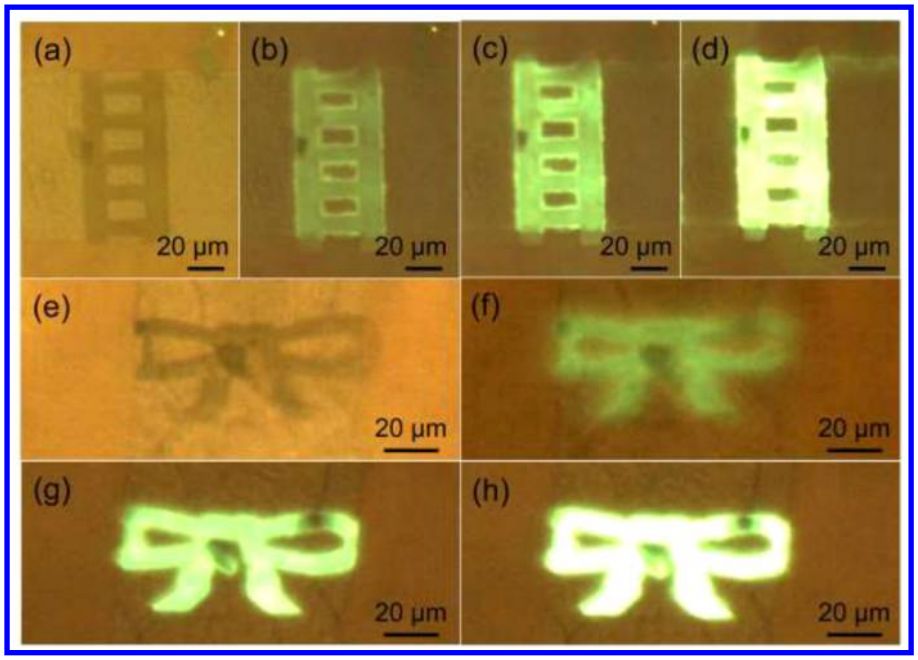

Figure 6. Optical microscopic images of operating micro-OLEDs based on the patterned RGO electrodes. (a–d) Ladder-shaped micro-OLED devices under different driving voltages of 0, 5, 7, and 9 V. (e–h) Bowknot-shaped micro-OLED devices under driving voltages of 0, 5, 7, and 9 V.

can be observed from the RGO side of the micro-OLEDs at a driving voltage of 5 V. Uniform and bright light is clearly observed, and the luminance increases with increasing driving voltage, as can be seen in Figure 6b–d. It is of interest to note that complex patterns such as bowknot-shaped micro-OLEDs could also be easily fabricated engaging the FsLDW reducing and patterning GO process as shown in Figure 6e–h. The bowknot-shaped micro-OLEDs also show well-defined shapes and edges and uniform EL emission in accordance with the ladder-shaped devices, indicating that micro-OLEDs with any desired patterns could be obtained based on FsLDW-reduced and patterned RGO electrodes.

CONCLUSIONS

We have successfully fabricated arbitrarily shape customized micro-OLEDs by using FsLDW-reduced and patterned GO film as the anode. According to the XPS, AFM images, and conductivity measurements, the GO film has been reduced and patterned synchronously through the mask-free Fs laser nanowriting pathway with high patterning resolution and good conduction characteristics. The micro-OLEDs with different patterns based on the FsLDW-induced RGO electrodes show well-defined sizes, shapes, and edges and uniform EL characteristics, which makes the micro-OLED devices more attractive in a wide range of scientific fields. Moreover, the application of the high-resolution and mask-free FsLDW technique in the reduction and patterning of GO might open up a new avenue for the design and fabrication of electronic and optoelectronic devices in the micro- or nanoscale.

MATERIALS AND METHODS

Preparation of Graphene Oxide. Graphene oxide is prepared by a modified Hummers method from natural graphite (Aldrich, <150 μm). Natural graphite powder (2 g) was mixed with $NaNO_3$ (2 g) and H_2SO_4 (96 mL) under stirring in an ice-bath. Then $KMnO_4$ (12 g) was added slowly into the mixed solution under stirring, and the temperature of the system was controlled at 0 °C. After 90 min the ice-bath was removed and the system was heated at 35 °C for 30 min. Then distilled water (80 mL) was slowly added into the system, and it was stirred for another 15 min. Then distilled water (200 mL) and a 3% H_2O_2 aqueous solution were added to reduce the residual $KMnO_4$ until the bubbling disappeared. Finally, the system was centrifuged at 12 000 rpm for 30 min, and the residue was washed with distilled water until the upper layer of the suspension reached a pH of ~7. The obtained sediment was redispersed into water and was treated by mild ultrasound for 15 min. A homogeneous suspension was collected after removing the trace black residues by centrifugation at 3000 rpm for 3 min. GO powder was obtained after freezing and drying of the suspension.[19] The GO powder was redispersed into water again, and the concentration of the GO solution was controlled at 1 mg/mL.

Femtosecond Laser Direct Writing Induced Reduction of GO. The femtosecond laser used to directly reduce and pattern GO was generated by Tsunami, Spectra-Physics lasers (model: 3960-X1BB s/n 2617; ccd: AMSTAR, B/W; video ccd: CAMERA). The Fs laser pulse with 790 nm central wavelength, 120 fs pulse width, and 80 MHz repetition rate was focused by a 100× objective lens with a high numerical aperture (NA = 1.4) into the GO film. The focal spot of the laser beam was scanned laterally by steering a two-galvano-mirror set and was vertically moved along the optical axis by a piezostage. A 10 mW laser power measured before the objective lens, a 600 μs exposure duration of each voxel, and a 100 nm scanning step length were adopted. It took around 6–7 min to produce the FsLDW-reduced GO films with a ladder or bowknot shape according to the above conditions.

Fabrication and Evaluation of micro-OLEDs Based on FsLDW-Reduced and Patterned GO Electrodes. Glass substrates were cleaned by acetone, ethanol, and ultrapure water, respectively. The GO film was spin-coated on the precleaned substrate at 3000 rpm and baked at 40 °C in a vacuum oven for 30 min. Then it was immediately loaded into a

dx.doi.org/10.1021/ph500106f | ACS Photonics 2014, 1, 690–695

thermal evaporation chamber. A 20 nm Au film as the extraction electrode was deposited on the prepared substrates with a 75 μm channel by using a shadow mask. The GO film was reduced and patterned in the channel by FsLDW. A 30 nm hole-injection layer of 4,4′,4″-tris(*N*-3-methylphenyl-*N*-phenylamino)triphenylamine (m-MTDATA), a 20 nm thick hole-transporting layer of *N*,*N*′-diphenyl-*N*,*N*′-bis(1,1′-biphenyl)-4,4′-diamine (NPB), a 50 nm emitting layer of tris(8-hydroxyquinoline)aluminum (Alq_3), and a cathode of LiF (1 nm)/Al (100 nm) were evaporated sequentially at a base pressure of 5×10^{-4} Pa. The OLEDs were driven by a Keithley 2400 programmable voltage−current source. Optical microscope images were obtained from a Motic BE400 microscope. The measurements were conducted in air at room temperature.

Fabrication and Evaluation of the RGO FET. Glass substrates coated with ITO film as the gate electrodes were precleaned. To obtain a gate dielectric layer, a poly(methyl methacrylate) (PMMA) chloroform solution (100 mg/mL) was spin-coated on the substrates at 3000 rpm and baked at 95 °C for 6 h and 120 °C for 2 h. The thickness of the PMMA was measured to be 200 nm. GO films were spin-coated on the PMMA layer and annealed at 40 °C in a vacuum oven for 30 min. Au source and drain electrodes were deposited onto the GO film under vacuum by using a shadow mask. In order to modulate the active layer, the GO film was then reduced and patternd into a 35 μm width belt between the electrodes (distance, 75 μm) for testing. Current−voltage curves of the FET were measured by a Keithley SCS 4200 semiconductor characterization system. The measurements were conducted in air at room temperature.

AUTHOR INFORMATION

Corresponding Authors

*E-mail: jingfeng@jlu.edu.cn.
*E-mail: yonglaizhang@jlu.edu.cn

Notes

The authors declare no competing financial interest.

ACKNOWLEDGMENTS

The authors gratefully acknowledge the financial support from the 973 Project (2013CBA01700) and NSFC (Grant Nos. 61322402, 91233123, and 61177024), and Graduate Innovation Fund of Jilin University (2014022).

REFERENCES

(1) Matsunaga, D.; Tamaki, T.; Akiyama, H.; Ichimura, K. Photofabrication of micro-patterned polarizing elements for stereoscopic displays. *Adv. Mater.* **2002**, *14*, 1477−1480.

(2) Deganello, D.; Cherry, J. A.; Gethin, D. T.; Claypole, T. C. Patterning of micro-scale conductive networks using reel-to-reel flexographic printing. *Thin Solid Films* **2010**, *518*, 6113−6116.

(3) Hoshino, K.; Hasegawa, T.; Matsumoto, K.; Shimoyama, I. Organic light-emitting diode micro patterned with a silicon convex stamp. *Sens. Actuators, A* **2006**, *128*, 339−343.

(4) Noach, S.; Faraggi, E. Z.; Cohen, G.; Avny, Y.; Neumann, R.; Davidov, D.; Lewis, A. Microfabrication of an electroluminescent polymer light emitting diode pixel array. *Appl. Phys. Lett.* **1996**, *69*, 3650−3652.

(5) Yamamoto, H.; Wilkinson, J.; Long, J. P.; Bussman, K.; Christodoulides, J. A.; Kafafi, Z. H. Nanoscale organic light-emitting diodes. *Nano Lett.* **2005**, *5*, 2485−2488.

(6) Boroumand, F. A.; Fry, P. W.; Lidzey, D. G. Nanoscale conjugated-polymer light-emitting diodes. *Nano Lett.* **2004**, *5*, 67−71.

(7) Li, S.-Q.; Guo, P.; Buchholz, D. B.; Zhou, W.; Hua, Y.; Odom, T. W.; Ketterson, J. B.; Ocola, L. E.; Sakoda, K.; Chang, R. P. H. Plasmonic−photonic mode coupling in indium-tin-oxide nanorod arrays. *ACS Photonics* **2014**, *1*, 163−172.

(8) Loo, Y.-L.; Willett, R. L.; Baldwin, K. W.; Rogers, J. A. Additive, nanoscale patterning of metal films with a stamp and a surface chemistry mediated transfer process: applications in plastic electronics. *Appl. Phys. Lett.* **2002**, *81*, 562−564.

(9) Childs, W. R.; Nuzzo, R. G. Large-area patterning of coinage-metal thin films using decal transfer lithography. *Langmuir* **2004**, *21*, 195−202.

(10) Park, S. K.; Kim, Y.-H.; Han, J.-I. High-resolution patterned nanoparticulate Ag electrodes toward all printed organic thin film transistors. *Org. Electron.* **2009**, *10*, 1102−1108.

(11) Li, Z.-H.; Cho, E. S.; Kwon, S. J. Laser direct patterning of the T-shaped ITO electrode for high-efficiency alternative current plasma display panels. *Appl. Surf. Sci.* **2010**, *257*, 776−780.

(12) Chae, J.; Jain, K. Excimer laser projection photoablation patterning of metal thin films for fabrication of microelectronic devices and displays. *IEEE Photon. Technol. Lett.* **2008**, *20*, 1216−1218.

(13) Guo, Q.; Zhu, H.; Liu, F.; Zhu, A. Y.; Reed, J. C.; Yi, F.; Cubukcu, E. Silicon-on-glass graphene-functionalized leaky cavity mode nanophotonic biosensor. *ACS Photonics* **2014**, *1*, 221−227.

(14) Huang, X.; Zeng, Z.; Fan, Z.; Liu, J.; Zhang, H. Graphene-based electrodes. *Adv. Mater.* **2012**, *24*, 5979−6004.

(15) Zhang, Y.; Guo, L.; Wei, S.; He, Y.; Xia, H.; Chen, Q.; Sun, H.-B.; Xiao, F.-S. Direct imprinting of microcircuits on graphene oxides film by femtosecond laser reduction. *Nano Today* **2010**, *5*, 15−20.

(16) Guo, L.; Jiang, H.-B.; Shao, R.-Q.; Zhang, Y.-L.; Xie, S.-Y.; Wang, J.-N.; Li, X.-B.; Jiang, F.; Chen, Q.-D.; Zhang, T.; Sun, H.-B. Two-beam-laser interference mediated reduction, patterning and nanostructuring of graphene oxide for the production of a flexible humidity sensing device. *Carbon* **2012**, *50*, 1667−1673.

(17) García de Abajo, F. J. Graphene plasmonics: challenges and opportunities. *ACS Photonics* **2014**, *1*, 135−152.

(18) Lee, Y.-Y.; Tu, K.-H.; Yu, C.-C.; Li, S.-S.; Hwang, J.-Y.; Lin, C.-C.; Chen, K.-H.; Chen, L.-C.; Chen, H.-L.; Chen, C.-W. Top laminated graphene electrode in a semitransparent polymer solar cell by simultaneous thermal annealing/releasing method. *ACS Nano* **2011**, *5*, 6564−6570.

(19) Wu, J.; Agrawal, M.; Becerril, H. A.; Bao, Z.; Liu, Z.; Chen, Y.; Peumans, P. Organic light-emitting diodes on solution-processed graphene transparent electrodes. *ACS Nano* **2009**, *4*, 43−48.

(20) Parvez, K.; Li, R.; Puniredd, S. R.; Hernandez, Y.; Hinkel, F.; Wang, S.; Feng, X.; Müllen, K. Electrochemically exfoliated graphene as solution-processable, highly conductive electrodes for organic electronics. *ACS Nano* **2013**, *7*, 3598−3606.

(21) Mueller, T.; Xia, F.; Avouris, P. Graphene photodetectors for high-speed optical communications. *Nat. Photonics* **2010**, *4*, 297−301.

(22) Parand, P.; Samadpour, M.; Esfandiar, A.; Iraji Zad, A. Graphene/PbS as a novel counter electrode for quantum dot sensitized solar cells. *ACS Photonics* **2014**, *1*, 323−330.

(23) Li, P.; Wong, M.; Zhang, X.; Yao, H.; Ishige, R.; Takahara, A.; Miyamoto, M.; Nishimura, R.; Sue, H.-J. Tunable lyotropic photonic liquid crystal based on graphene oxide. *ACS Photonics* **2013**, *1*, 79−86.

(24) Guo, L.; Shao, R.-Q.; Zhang, Y.-L.; Jiang, H.-B.; Li, X.-B.; Xie, S.-Y.; Xu, B.-B.; Chen, Q.-D.; Song, J.-F.; Sun, H.-B. Bandgap tailoring and synchronous microdevices patterning of graphene oxides. *J. Phys. Chem. C* **2012**, *116*, 3594−3599.

(25) Zhang, Y.-L.; Chen, Q.-D.; Xia, H.; Sun, H.-B. Designable 3D nanofabrication by femtosecond laser direct writing. *Nano Today* **2010**, *5*, 435−448.

(26) Gao, W.; Singh, N.; Song, L.; Liu, Z.; Reddy, A. L. M.; Ci, L.; Vajtai, R.; Zhang, Q.; Wei, B.; Ajayan, P. M. Direct laser writing of micro-supercapacitors on hydrated graphite oxide films. *Nat. Nano* **2011**, *6*, 496−500.

(27) Sun, Y.-L.; Dong, W.-F.; Yang, R.-Z.; Meng, X.; Zhang, L.; Chen, Q.-D.; Sun, H.-B. Dynamically tunable protein microlenses. *Angew. Chem. Int. Ed* **2012**, *124*, 1590−1594.

(28) Lee, B. R.; Kim, J.-w.; Kang, D.; Lee, D. W.; Ko, S.-J.; Lee, H. J.; Lee, C.-L.; Kim, J. Y.; Shin, H. S.; Song, M. H. Highly efficient polymer light-emitting diodes using graphene oxide as a hole transport layer. *ACS Nano* **2012**, *6*, 2984−2991.
(29) Chen, W.; Yan, L. Centimeter-sized dried foam films of graphene: preparation, mechanical and electronic properties. *Adv. Mater.* **2012**, *24*, 6229−6233.
(30) Wei, Z.; Wang, D.; Kim, S.; Kim, S.-Y.; Hu, Y.; Yakes, M. K.; Laracuente, A. R.; Dai, Z.; Marder, S. R.; Berger, C.; King, W. P.; de Heer, W. A.; Sheehan, P. E.; Riedo, E. Nanoscale tunable reduction of graphene oxide for graphene electronics. *Science* **2010**, *328*, 1373−1376.
(31) Zhang, Y.-L.; Guo, L.; Xia, H.; Chen, Q.-D.; Feng, J.; Sun, H.-B. Photoreduction of graphene oxides: methods, properties, and applications. *Adv. Opt. Mater.* **2014**, *2*, 10−28.
(32) Wang, J.-N.; Shao, R.-Q.; Zhang, Y.-L.; Guo, L.; Jiang, H.-B.; Lu, D.-X.; Sun, H.-B. Biomimetic graphene surfaces with superhydrophobicity and iridescence. *Chem.—Asian J.* **2012**, *7*, 301−304.
(33) Wan, D.; Yang, C.; Lin, T.; Tang, Y.; Zhou, M.; Zhong, Y.; Huang, F.; Lin, J. Low-temperature aluminum reduction of graphene oxide, electrical properties, surface wettability, and energy storage applications. *ACS Nano* **2012**, *6*, 9068−9078.